Accepted Manuscript

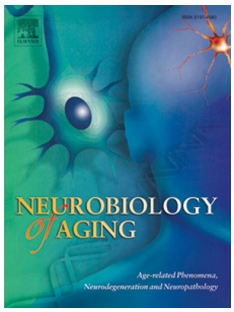

Genetically reducing mTOR signaling rescues central insulin dysregulation in a mouse model of Alzheimer's disease

Antonella Caccamo, Ramona Belfiore, Salvatore Oddo

PII: S0197-4580(18)30121-0

DOI: 10.1016/j.neurobiolaging.2018.03.032

Reference: NBA 10213

To appear in: *Neurobiology of Aging*

Received Date: 20 September 2017

Revised Date: 28 March 2018

Accepted Date: 29 March 2018

Please cite this article as: Caccamo, A., Belfiore, R., Oddo, S., Genetically reducing mTOR signaling rescues central insulin dysregulation in a mouse model of Alzheimer's disease, *Neurobiology of Aging* (2018), doi: 10.1016/j.neurobiolaging.2018.03.032.

Genetically reducing mTOR signaling rescues central insulin dysregulation in a mouse model of Alzheimer's disease

Antonella Caccamo[1], Ramona Belfiore[1, 2], and Salvatore Oddo[1, 3, #]

[1]The Arizona State University-Banner Neurodegenerative Disease Research Center at the Biodesign Institute, Arizona State University, Tempe, Arizona, 85287.

[2]Department of Biomedical and Biotechnological Sciences, University of Catania, Catania, Italy, 95125

[3]School of Life Sciences, Arizona State University, Tempe, Arizona, 85287

Authors' email addresses:
Antonella Caccamo (caccamo@asu.edu)
Ramona Belfiore (rbelfior@asu.edu)
Salvatore Oddo (oddo@asu.edu)

[#]*To whom correspondence should be addressed:*

SALVATORE ODDO, Ph.D.
The Arizona State University-Banner Neurodegenerative Disease Research Center
Biodesign Institute
School of Life Sciences
Arizona State University
1001 S. McAllister Ave
Tempe, AZ 85287-5001
480-727-3490
oddo@asu.edu

ABBREVIATIONS

AD: Alzheimer's disease. **Aβ:** Amyloid-β. **IGF:** insulin growth factor. **IGFR-1:** insulin growth factor receptor-1. **IRs:** insulin receptors. **IRS-1:** insulin receptor substrate-1. **mTOR:** mammalian target of rapamycin. **S6K1:** ribosomal protein S6 kinase 1. **T2D:** type two diabetes.

ABSTRACT

Alzheimer's disease (AD) is the most common neurodegenerative disease. The causes of sporadic AD, which represents more than 95% of AD cases, are unknown. Several AD risk factors have been identified and among these, type two diabetes increases the risk of developing AD by two-fold. However, the mechanisms by which diabetes contributes to AD pathogenesis remain elusive. The mammalian target of rapamycin (mTOR) is a protein kinase that plays a crucial role in the insulin signaling pathway and has been linked to AD. We used a crossbreeding strategy to remove one copy of the mTOR gene from the forebrain of Tg2576 mice, a mouse model of AD. We used 20-month-old mice to assess changes in central insulin signaling and found that Tg2576 mice had impaired insulin signaling. These impairments were mTOR dependent as we found an improvement in central insulin signaling in mice with lower brain mTOR activity. Further, removing one copy of mTOR from Tg2576 mice improved cognition and reduced levels of Aβ, tau, and cytokines. Our findings indicate that mTOR signaling is a key mediator of central insulin dysfunction in Tg2576. These data further highlight a possible role for mTOR signaling in AD pathogenesis and add to the body of evidence indicating that reducing mTOR activity could be a valid therapeutic approach for AD.

INTRODUCTION

The prevalence of Alzheimer's disease (AD) and type two diabetes (T2D) is growing at an alarming pace (Alzheimer's, 2016; Menke et al., 2015). Clinically, AD is associated with memory loss and alterations in other cognitive domains that eventually lead patients to be bedridden (Lambon Ralph et al., 2003; Perry and Hodges, 1999). While the etiology of AD remains unknown, the accumulation of amyloid-β and tau and the development of neuroinflammation are key neuropathological hallmarks of AD (Querfurth and LaFerla, 2010). T2D leads to extensive systemic alteration affecting multiple organs including heart, kidneys, and eyes (Trikkalinou et al., 2017). While several prominent risk factors for T2D have been identified, dysregulation of insulin signaling is a critical event in the disease pathogenesis (Sims-Robinson et al., 2010).

Multiple epidemiological studies have indicated that diabetes increases the risk of developing AD by about 2-fold (Ott et al., 1999; Sims-Robinson et al., 2010). Consistent with these observations, biochemical and neuropathological examinations have indicated insulin dysregulation in human AD tissue and animal models of AD (Pedersen and Flynn, 2004; Rodriguez-Rivera et al., 2011; Vandal et al., 2015). This type of evidence has led to the hypothesis that central and peripheral metabolic dysfunctions are linked to AD pathogenesis (Diehl et al., 2017; Kandimalla et al., 2017; Shinohara and Sato, 2017). Despite this wealth of information, the molecular mechanisms underlying the interaction between AD and T2D remain elusive.

The mammalian target of rapamycin (mTOR) is a protein kinase that regulates cell growth and proliferation, as well as protein turnover via autophagy (Saxton and Sabatini, 2017). Under physiological conditions, mTOR is activated by several signaling pathways, including in response to activation of the insulin receptors (IRs) and the insulin growth factor receptor-1 (IGFR-1) (Saxton and Sabatini, 2017). A key mediator of mTOR function is the ribosomal

protein S6 kinase 1 (S6K1), which is activated following direct phosphorylation by mTOR (Magnuson et al., 2012). While physiological activation of mTOR signaling positively regulates insulin signaling, chronic hyperactivation of mTOR, which is a hallmark of T2D, exacerbates insulin resistance and contributes to the development of T2D (Suhara et al., 2017). These apparent paradoxical events are linked to a negative feedback loop in which hyperactive S6K1 phosphorylates the insulin receptor substrate-1 (IRS-1), thereby leading to the internalization of the receptor and insulin resistance (Um et al., 2004).

Growing evidence indicates that mTOR is also hyperactive in AD (An et al., 2003; Caccamo et al., 2015; Chang et al., 2002; Oddo, 2012; Pei et al., 2008; Pei and Hugon, 2008). For example, Pei and colleagues reported that in postmortem human brains, mTOR/S6K1 signaling pathway is hyperactive in brain regions affected by the disease (An et al., 2003). We have confirmed these data using a different cohort of human patients (Caccamo et al., 2015). Hyperactive mTOR signaling has also been reported in multiple animal models of AD, including in Tg2575 mice (Caccamo et al., 2014). Using complementary genetic and pharmacological approaches, we and others have shown that reducing hyperactive mTOR ameliorates cognitive deficits and reduces Aβ and tau pathology in multiple animal models of AD (Caccamo et al., 2015; Caccamo et al., 2014; Caccamo et al., 2013; Caccamo et al., 2010; Caccamo et al., 2011; Majumder et al., 2011; Spilman et al., 2010). In this study, we sought to determine the role of brain mTOR signaling on central insulin dysregulation associated with AD.

METHODS AND MATERIALS

Mice: Floxed mTOR mice contain LoxP sites flanking exons 49 and 50 of the mTOR gene; the generation of these mice has been previously described (Lang et al., 2010). Tg2576, APP/mTOR$^{+/-}$ and mTOR floxed mice used in this manuscript were previously described (Caccamo et al., 2014; Hsiao et al., 1995). We have previously described the breeding strategy

employed to obtain the mice used here (Caccamo et al., 2014). Briefly, to remove one copy of the mTOR gene from the brains of Tg2576 mice, we first bred hemizygous Tg2576 mice with homozygous mice expressing the Cre recombinase under the control of the CamKII promoter. From these breeding, we obtained Tg2576 mice expressing one copy of Cre, which were then bred with homozygous mTOR floxed mice to obtain the mice used in this study, which were all littermates. We used both females and males for this study. Mice were housed 4-5 per cage and kept on 12-hour light/dark cycle. Mice were 20-month-old at the beginning of the experiments. Mice were given *ad libitum* access to food and water. All animal procedures were approved by The Institutional Animal Care and Use Committee of Arizona State University.

Morris water maze: The Morris water maze was used to assess spatial learning and memory. It was performed in a circular plastic tank of 1.5 m diameter. The tank was filled with opaque water kept at 23°C. A platform of 14 cm wide was held just 1.5 cm under the surface of the water. To make the platform invisible to the mice, the water was made opaque by non-toxic paint. Extramazal cues were located throughout the room to allow the mice to find the escape platform. Mice were given four training trials of 60 seconds each per day for five consecutive days. Twenty-four hours after the last training trial, the platform was removed and a single 60 seconds probe trial to assess spatial memory was conducted. A video camera positioned on the ceiling was utilized to record the entire test. A tracking software (EthoVision XT, Noldus) was used to analyze the data.

Protein extraction: Brains were processed as described previously (Caccamo et al., 2017). Briefly, for biochemical analyses, mice were sacrificed by CO_2 asphyxiation, their brains removed and sagittally bisected. The cortex was removed and homogenized in T-PER protein extraction buffer (Thermo Fisher, Waltham, MA; catalog number 78510), containing complete protease inhibitor (Roche, Indianapolis, IN; catalog number 11836153001) and phosphatase

inhibitor (Thermo Fisher, Waltham, MA; catalog number 524625). The homogenates were centrifuged at 4 °C for 30 minutes at 25,000 × *g*. The supernatant was stored at -80 °C and used for ELISA and western blots. The pellet was re-suspended in 70% formic acid and used as insoluble fraction.

Western blot: The soluble protein extracts were loaded on SDS/PAGE precast gels (Thermo Fisher, Waltham, MA; catalog number WG1203BOX) and ran under reducing condition as we described before (Branca et al., 2014). Briefly, samples were boiled in loading buffer at 100 °C for 5 minutes to denature proteins. Proteins were transferred to a nitrocellulose membrane and incubated for 1 hour in 5% milk in T-TBS (0.1% Tween 20, 100 mM Tris, pH 7.5; 150 mM NaCl. These reagents were purchased from Thermo Fisher Scientific: Catalog numbers BP337-500, BP152-5, and BP358-10, respectively. Then, membranes were washed and incubated overnight at 4 °C and incubated in secondary anti-rabbit or anti-mouse HRP antibodies (1:10,000; these reagents were purchased from Thermo Fisher Scientific, catalog numbers 31460 and 31430, respectively) in blocking buffer at room temperature for 1 hour. Images were acquired with a developer machine using a chemiluminescent solution (Thermo Fisher, Waltham, MA; catalog number 34076).

ELISAs: IGF1, p-IGF1, $A\beta_{40}$ and $A\beta_{42}$ levels were assessed via sandwich ELISA using commercially available kits (Thermo Fisher, Waltham, MA; catalog number: EMIGF1, LHO0501, KHB3481 and KHB3442, respectively) per the manufacturer's instructions.

Antibodies: The following antibodies were used for western blots: from Cell Signaling, Danvers, MA: total mTOR (1:1000; catalog number 2983S), total S6K1 (1:1000; catalog number 9202S), pS6K1 Thr389 (1:1000; catalog number 9205S), β-actin (1:10000; catalog number 3700S), total IRS-1 (1:1000; catalog number 3407S), IRS Ser318 (1:1000; catalog number 5610S), IRS

Ser636/639 (1:1000; catalog number 2388S), totalPI3K p85 (1:1000; catalog number 4292S), PI3K Tyr458 (1:1000; catalog number 4228S), total AKT (1:1000 ; catalog number 9272), AKT Thr308 (1:1000; catalog number 2965S), AKT Ser473 (1:1000; catalog number3787S) total GSK3β (1:1000; catalog number 9315S), GSK3β Ser9 (1:1000; catalog number 9336S), CP13 (1:1000; catalog number 11834S). From Millipore, Billerica, MA: APP C-terminal (1:2000; catalog number 171610), Tau5 (1:5000; catalog number 577801). From BioLegend, San Diego, CA: APP (1:3000; catalog number MAB348). PHF-1 (1:3000) was a gift from Dr. Peter. Davies.

Statistical analysis: While both sexes were used, the experiments were not powered to identify sex differences. For western blots and the ELISA experiments, the cortex of each mouse was processed as indicated above. Each statistical replicate represents proteins extracted from one mouse. Per each mouse, all the western blots were obtained from the same homogenate. Normality was tested via the D'Agostino & Pearson omnibus normality test (*p*'s > 0.20). Data were analyzed by one-way and two-way ANOVAs using GraphPad Prism. *Post hoc* Bonferroni's test was then used to determine individual differences among groups.

RESULTS

Reduced mTOR levels and signaling in the cortex of aged APP/mTOR$^{+/-}$ mice

Using mTOR floxed mice and a CamKII-Cre line, we have removed one copy of the mTOR gene from the brains of Tg2576 mice using a crossbreeding approach (Caccamo et al., 2014). In this study, we used 20-month-old littermates with the following genotypes: Tg2576$^{+/0}$;mTOR$^{wt/fl}$;CRE$^{0/0}$ (herein referred to as APP mice); Tg2576$^{+/0}$;mTOR$^{wt/fl}$;CRE$^{+/0}$ (herein referred to as APP/mTOR$^{+/-}$ mice); Tg2576$^{0/0}$;mTOR$^{wt/fl}$;CRE$^{0/0}$ (herein referred to as CTL mice); Tg2576$^{0/0}$;mTOR$^{wt/fl}$;CRE$^{+/0}$ (herein referred to as mTOR$^{+/-}$ mice). + indicates the presence of the transgene, 0 indicates the lack of the transgene, fl indicates a floxed mTOR allele, wt indicates a

wildtype mTOR allele. To determine the effects of removing one copy of the mTOR gene on learning and memory, we tested mice in the Morris water maze (MWM; n = 10/genotype). We started by training mice (four training trials per day per five consecutive days) to find a hidden platform using extra-maze cues. When we analyzed the time to find the hidden platform using a two-way ANOVA, we found a significant effect for days [$p < 0.0001$; $F_{(4, 170)} = 20.34$], genotype [$p = 0.0008$; $F_{(3, 170)} = 10.18$], and day x genotype interaction [$p = 0.047$; $F_{(12, 170)} = 2.51$; Fig. 1A]. The day effect indicates that all mice learned the task across the five days of training. The genotype effect indicates that one or more genotypes had a different pace of learning. Post hoc analyses indicated that APP/mTOR$^{+/-}$ mice performed significantly better than APP mice at day 4 ($p < 0.05$, $t = 2.76$) and day 5 ($p < 0.01$, $t = 3.28$). Twenty-four hours after the last training trial, we removed the platform from the maze and conducted probe trials to assess spatial memory during a single 60-second probe trial. We found that the number of platform location crosses was significantly different among the four genotypes [$p < 0.0001$; $F_{(3, 34)} = 11.18$; Fig. 1B). *Post-hoc* analyses indicated that APP mice performed significantly worse compared to CTL ($p < 0.01$; $t = 5.47$), mTOR ($p < 0.01$; $t = 4.21$), and APP/mTOR$^{+/-}$ mice ($p < 0.01$; $t = 3.70$). We then analyzed the latency to the first platform cross and found that there was a significant difference among the groups [$p < 0.0001$; $F_{(3, 34)} = 22.86$; Fig. 1C]. *Post-hoc* analyses indicated that APP mice performed significantly worse compared to CTL ($p < 0.01$; $t = 7.57$), mTOR ($p < 0.01$; $t = 6.40$), and APP/mTOR$^{+/-}$ mice ($p < 0.01$; $t = 5.57$). Notably, swim speed was not statistically significant among the four groups (Fig. 1D), suggesting that the performance deficits are not due to motor issues. These data indicate that the APP mice are significantly impaired compared to CTL mice in all three measurements (Fig. 1A-C), and removing one copy of the mTOR gene rescues these deficits.

To better understand the relationship between mTOR and central insulin resistance in AD, we first measured the body weight of mice before we sacrificed them and found that there was no

statistically significant difference among the four groups (p = 0.4028; Fig. 2A). To assess mTOR signaling, we measured mTOR levels by western blot. We found that mTOR levels were significantly different among the four genotypes [$p < 0.001$; $F_{(3, 16)} = 36.62$; Fig. 2B-C]. Specifically, a *post hoc* test with Bonferroni's correction showed that the total levels of mTOR were significantly higher in APP mice compared to CTL ($p < 0.01$; $t = 5.12$), mTOR ($p < 0.001$; $t = 8.57$), and APP/mTOR$^{+/-}$ mice ($p < 0.001$; $t = 9.65$). Also, mTOR levels in CTL mice were higher compared to mTOR$^{+/-}$ ($p < 0.05$; $t = 3.45$) and APP/mTOR$^{+/-}$ mice ($p < 0.05$; $t = 3.92$). Notably, no differences were found between mTOR$^{+/-}$ and APP/mTOR$^{+/-}$ mice. To further assess mTOR signaling, we measured the total and phosphorylated levels of S6K1, a protein downstream of mTOR (Fenton and Gout, 2011). While overall levels of S6K1 were similar among the four groups (p = 0.3084; Fig. 2B-D), we found that the levels of S6K1 phosphorylated at Thr389 were significantly different [$p = 0.0051$; $F_{(3, 16)} = 7.20$; Fig. 2B-E]. A *post hoc* test with Bonferroni's correction showed that phosphorylated levels of S6K1 were significantly higher in the APP mice compared to CTL ($p < 0.01$; $t = 4.13$), mTOR$^{+/-}$ ($p < 0.05$; $t = 3.47$), and APP/mTOR$^{+/-}$ ($p < 0.05$; $t = 3.65$) mice. These data show that genetically removing one copy of mTOR from the brain of Tg2576 mice is sufficient to reduce mTOR levels and signaling.

Removing one copy of mTOR rescues aberrant brain insulin signaling

mTOR hyperactivity is linked to insulin resistance, hyperglycemia and hyperinsulinemia in the periphery (Suhara et al., 2017); however, whether brain mTOR plays a role in central insulin metabolism remains to be elucidated. To explore the effect of genetically reducing mTOR on central insulin signaling, we measured the levels of the insulin receptor β (IRβ) by western blot. IRs are highly expressed in neurons and are downregulated in AD brains (Schulingkamp et al., 2000; Steen et al., 2005). We found that the levels of IRβ were different among the groups [$p < 0.0001$; $F_{(3, 16)} = 37.86$; Fig. 3A-B). A *post hoc* test with Bonferroni's correction showed that the

levels of IRβ were lower in APP mice compared to CTL ($p < 0.001$; $t = 7.74$), $mTOR^{+/-}$ ($p < 0.001$; $t = 7.30$), and $APP/mTOR^{+/-}$ ($p < 0.001$; $t = 9.71$) mice. To further investigate changes in central insulin signaling, we focused on the insulin receptor substrate (IRS). IRS-1 is a regulator of insulin signaling, and its phosphorylation at serine residues can positively or negatively regulate insulin signaling (Boura-Halfon and Zick, 2009; Gual et al., 2005). For example, IRS-1 phosphorylated at Ser318 by PKCζ immediately after exposure to insulin facilitates insulin signaling by stimulating the activation of the PI3K/AKT pathway (Boura-Halfon and Zick, 2009; Gual et al., 2005). Furthermore, phosphorylation at Ser636/639 always inhibits and disrupts insulin signaling (Gual et al., 2005; Spilman et al., 2010). We measured the steady-state levels of total IRS-1 and found no difference among the four groups ($p = 0.9118$; Fig. 3B-C). In addition, we found that the levels of IRS-1 phosphorylated at Ser318 and 636/639 were different among the four genotypes [$p = 0.0093$; $F_{(3, 16)} = 7.17$ and $p = 0.0304$; $F_{(3, 16)} = 4.53$, respectively; Fig. 3A, D-E]. A *post hoc* test with Bonferroni's correction showed that the levels of IRS-1 phosphorylated at Ser318 and 636/639 were higher in APP mice compared to CTL ($p < 0.05$; $t = 4.02$ and $p < 0.05$; $t = 3.15$, respectively), $mTOR^{+/-}$ ($p < 0.05$; $t = 3.95$ and $p < 0.05$; $t = 3.82$, respectively), and $APP/mTOR^{+/-}$ mice ($p < 0.05$; $t = 3.43$ and $p < 0.05$; $t = 3.20$, respectively).

IGF-1R is tetrameric glycoprotein that belongs to the receptor tyrosine kinase superfamily, which can be activated by insulin and IGF-1 (Hernandez-Sanchez et al., 1995). Phosphorylation of IGF-1R at Tyr1135/1136 is necessary for kinase activation, and it is one of the earliest cellular responses to insulin. In mouse models of AD, the disruption of insulin/IGF signaling increases Aβ deposition, tau phosphorylation, and decreases cerebral blood flow (de la Monte, 2012; Ke et al., 2009; Talbot et al., 2012). To study this specific aspect of insulin signaling, we measured the levels of total IGF-1R by ELISA and found that they were significantly different among the four groups ($p < 0.0001$; $F_{(3, 16)} = 37.81$; Fig. 3F). A *post hoc* test with Bonferroni's

correction showed that IGF-1R levels were lower in APP mice compared to CTL ($p < 0.001$; $t = 8.40$), $mTOR^{+/-}$ ($p < 0.001$; $t = 8.08$), and $APP/mTOR^{+/-}$ ($p < 0.001$; $t = 9.40$) mice. Consistent with these results, we found that the levels of IGF-1R phosphorylated at Tyr1135/1136 were also significantly different among the four groups ($p = 0.0033$; $F_{(3, 16)} = 37.81$; Fig. 3G). *Post hoc* analyses indicated that this difference was driven by the APP mice, which had the lowest levels of IGF-1R phosphorylated at Tyr1135/1136 compared to CTL ($p < 0.05$; $t = 3.20$), $mTOR^{+/-}$ ($p < 0.001$; $t = 4.35$), and $APP/mTOR^{+/-}$ mice ($p < 0.05$; $t = 3.22$). Taken together, these results show that reducing brain mTOR signaling rescues metabolic alterations in the central insulin signaling.

Reducing mTOR expression rescues the aberrant activation of the PI3K/AKT signaling

The pathway linking IRS proteins to the metabolic actions of insulin and insulin growth factors (IGF) is the PI3-kinase (PI3K)/AKT pathway (Gual et al., 2005; Hernandez-Sanchez et al., 1995). After insulin and IGF bind to IGFR-1 or to IRs, the PI3K/AKT pathway is activated and triggers a signaling transduction pathway that culminates with the phosphorylation at Thr308 and activation of AKT (Boura-Halfon and Zick, 2009; Gual et al., 2005). mTOR-mediated phosphorylation of AKT at Ser473 stimulates its full enzymatic activity (Hresko and Mueckler, 2005). To determine if reducing mTOR signaling modifies this signaling pathway downstream of IRS-1, we first measured the levels of total PI3K by western blot. We found that there was no difference among the four genotypes ($p = 0.7921$: Fig. 4A-B). In contrast, when we measured the levels of PI3K phosphorylated at Tyr458, we found a statistically significant difference among the four groups ($p = 0.0036$; $F_{(3, 16)} = 11.01$; Fig. 4A, C). A *post hoc* test with Bonferroni's correction showed that the levels of phosphorylated PI3K were higher in the APP mice compared to CTL ($p < 0.01$; $t = 4.87$), $mTOR^{+/-}$ ($p < 0.001$; $t = 4.95$), and $APP/mTOR^{+/-}$ mice ($p < 0.01$; $t = 4.04$). To investigate if changes in phosphorylated PI3K would affect its downstream targets, we measured the levels of total and phosphorylated AKT. While total AKT levels were

similar among the four groups (Fig. 4A, D), we found that the levels of AKT phosphorylated at Thr308 and Ser473 were significantly different among the four genotypes ($p = 0.0063$; $F_{(3, 16)} = 5.86$ and $p = 0.0075$; $F_{(3, 16)} = 6.45$, respectively; Fig. 4A, E-F). A *post hoc* test with Bonferroni's correction showed that the levels of AKT phosphorylated at Thr308 and Ser473 were higher in APP mice compared to CTL ($p < 0.05$; $t = 4.09$ and $p < 0.05$; $t = 3.38$, respectively), $mTOR^{+/-}$ ($p < 0.05$; $t = 3.37$ and $p < 0.05$; $t = 3.62$, respectively), and $APP/mTOR^{+/-}$ mice ($p < 0.05$; $t = 3.70$ and $p < 0.05$; $t = 3.74$, respectively). Taken together, these data indicate that 20-month-old APP mice have abnormal central insulin signaling, and these alterations were rescued by reducing brain mTOR signaling.

Reducing mTOR signaling lowers Aβ and tau levels in Tg2576 mice

Brain insulin resistance has been implicated as a key factor in the development of AD pathology (de la Monte, 2012; Diehl et al., 2017; Kandimalla et al., 2017). To evaluate the effect of lowering mTOR signaling on Aβ, we first measured Aβ load in cortical sections of APP and $APP/mTOR^{+/-}$ mice, stained with an Aβ42-specific antibody. We found that Aβ deposits were significantly reduced in $APP/mTOR^{+/-}$ mice compared to APP mice ($p < 0.0001$; $t = 12.99$; Fig. 5A-B). We also measured full-length APP and its major C-terminal fragments, C99 and C83, by western blot in the APP and $APP/mTOR^{+/-}$ mice. We found that the levels of APP, C99 and C83 were not statistically different between the two genotypes ($p = 0.183$, $p = 0.454$, and $p = 0.297$, respectively; Fig. 5C-F). Next, we measured soluble and insoluble Aβ levels by sandwich ELISA and found that soluble Aβ40 and Aβ42 levels were significantly reduced in the cortex of the $APP/mTOR^{+/-}$ mice compared to APP mice ($p = 0.0004$; $t = 5.71$ and $p = 0.0003$; $t = 6.00$, respectively; Fig. 5G). While the levels of insoluble Aβ40 were similar between the two groups, insoluble Aβ42 levels were lower in the $APP/mTOR^{+/-}$ mice compared to APP mice ($p = 0.0002$; $t = 6.13$; Fig 5H). These results show that reducing mTOR signaling is sufficient to reduce Aβ levels, without modifying APP processing. This finding is highly consistent with previous reports

(Caccamo et al., 2015; Caccamo et al., 2014; Caccamo et al., 2013; Caccamo et al., 2010; Majumder et al., 2011; Spilman et al., 2010).

Tau accumulation is another neuropathological feature of AD (Khurana et al., 2006). While Tg2576 mice do not develop frank neurofibrillary tau pathology, increases in tau phosphorylation have been reported (Sturchler-Pierrat et al., 1997). Furthermore, previous reports have indicated a direct link between mTOR and tau (Caccamo et al., 2015; Caccamo et al., 2014; Caccamo et al., 2013; Oddo, 2012). Hence, we looked at endogenous tau levels by western blot in all four groups of mice. We first measured total levels of endogenous tau and found a statistically significant difference among the four genotypes ($p = 0.0068$; $F_{(3, 16)} = 7.84$; Fig. 6A-B). A *post hoc* test with Bonferroni's correction showed that tau levels were higher in the APP mice compared to CTL ($p < 0.05$; $t = 4.00$), $mTOR^{+/-}$ ($p < 0.05$; $t = 3.87$), and $APP/mTOR^{+/-}$ mice ($p < 0.05$; $t = 3.98$). We next probed for changes in tau phosphorylation using two different phospho-specific tau antibodies: CP13, which recognizes tau phosphorylated at Ser202, and PHF-1, which recognizes tau phosphorylated at Ser396/404. We found that CP13 levels were significantly different in the four genotypes ($p < 0.001$; $F_{(3, 16)} = 12.42$; Fig. 6A, C). Interestingly, a *post hoc* test with Bonferroni's correction showed that the APP mice have the higher levels of phosphorylated tau compared to CTL ($p < 0.001$; $t = 5.60$), $mTOR^{+/-}$ ($p < 0.01$; $t = 4.25$), and $APP/mTOR^{+/-}$ mice ($p < 0.05$; $t = 4.75$). In contrast, we found that there were no statistically significant differences in PHF-1 levels among the four groups ($p = 0.1717$; Fig. 6A, D). To explore the mechanism of tau phosphorylation, we investigated levels of GSK3β, a tau kinase that has been involved in AD pathogenesis (Ma, 2014). *In vitro* and *in vivo* studies have shown that Aβ activates GSK3β, by preventing its inhibitory phosphorylation at Ser9. A similar increase in GSK3β activity has been detected in human AD brains. This increase in activity is believed to be involved in tau hyperphosphorylation and memory dysfunction (Kremer et al., 2011; Llorens-Martin et al., 2014). Further, GSK3β activity is linked to insulin signaling (Cross et al., 1995).

We found that the levels of total GSK3β were unchanged among the four genotypes ($p = 0.9770$; Fig. 6E). In contrast, the levels of GSK3β phosphorylated at Ser9 were different among the four groups ($p < 0.0001$; $F_{(3, 16)} = 34.54$; Fig. 6F). A *post hoc* test with Bonferroni's correction showed that the levels of GSK3β phosphorylated at Ser9 were lower in the APP mice compared to CTL ($p < 0.001$; $t = 9.11$), $mTOR^{+/-}$ ($p < 0.01$; $t = 7.60$), and $APP/mTOR^{+/-}$ mice ($p < 0.05$; $t = 3.23$). This finding indicates that GSK3β is hyperactive in APP mice compared to CTL mice and that decreasing mTOR levels restores GSK3β activity. While further studies are needed to address the mechanisms leading to GSK3β hyperactivity in APP mice, it is plausible that Aβ accumulation might play a key role in this process (Kremer et al., 2011; Llorens-Martin et al., 2014). In summary, lowering mTOR signaling in the brain of APP mice modifies insulin signaling and reduces GSK3β and tau phosphorylation.

Lowering mTOR levels reduces overproduction of cytokines

Overproduction of pro-inflammatory cytokines is a feature of AD and metabolic disorders, such as diabetes (Da Mesquita et al., 2016; King, 2008). To this end, brain inflammation has been linked to altered insulin signaling in AD and increase in tau phosphorylation (Kitazawa et al., 2004). To investigate the link between mTOR/insulin signaling and cytokines production, we measured the levels of and of IL1β and TNFα, two significant cytokines linked to AD (Kitazawa et al., 2004). We found that IL1β levels were different among the groups ($p = 0.0010$; $F_{(3, 16)} = 8.29$; Fig. 7A-B). A *post hoc* test with Bonferroni's correction showed that the levels of IL1β were higher in the APP compared to CTL ($p < 0.01$; $t = 4.11$), $mTOR^{+/-}$ ($p < 0.01$; $t = 4.33$), and $APP/mTOR^{+/-}$ mice ($p < 0.05$; $t = 3.65$). We found similar results when we analyzed TNFα levels ($p = 0.01$; $F_{(3, 16)} = 8.29$; Fig. 7A-C). A *post hoc* test with Bonferroni's correction showed that the levels of TNFα were higher in the APP compared to CTL ($p < 0.05$; $t = 3.61$), $mTOR^{+/-}$ ($p < 0.05$;

t = 3.68), and APP/mTOR$^{+/-}$ mice ($p < 0.05$; t = 3.62). These results show that lowering mTOR signaling and restoring insulin signaling reduces levels of toxic cytokines overproduction.

DISCUSSION

There is a clear and unchallenged link between diabetes and AD (Diehl et al., 2017; Kandimalla et al., 2017; Ott et al., 1999; Sims-Robinson et al., 2010). Consistent with these results, patients with diabetes and familial (caused by presenilin mutations) or sporadic AD had worse cognitive deficits compared to AD cases without diabetes (Abner et al., 2016; Aguirre-Acevedo et al., 2016). Abnormalities in insulin signaling have been consistently reported in human AD brains and animal models of AD (de la Monte, 2012; Diehl et al., 2017; Kandimalla et al., 2017; Ke et al., 2009; Pedersen and Flynn, 2004; Rodriguez-Rivera et al., 2011; Shinohara and Sato, 2017; Sims-Robinson et al., 2010; Talbot et al., 2012; Velazquez et al., 2017). For example, we recently reported that in Tg2576 mice, central insulin dysregulation proceeds peripheral insulin dysregulation; these changes are associated with alteration in brain energy metabolism (Velazquez et al., 2017). Despite this report, the mechanisms linking AD to insulin dysregulation remain unknown. Here we report the novel finding that hyperactive mTOR signaling contributes to insulin dysregulation in Tg2576 mice. This finding is consistent with our previous report showing that high sucrose diet alters central insulin signaling and exacerbates AD-like pathology in a mTOR-dependent manner (Orr et al., 2014).

We and others have previously shown that mTOR is hyperactive in postmortem human brains and in animal models of AD (An et al., 2003; Chang et al., 2002; Oddo, 2012; Pei et al., 2008; Pei and Hugon, 2008; Velazquez et al., 2017). mTOR phosphorylates and activates S6K1, which in turn phosphorylates the IRS-1 causing its internalization (Um et al., 2004). Chronic mTOR activation leads insulin resistance (Um et al., 2006). Consistent with these observations, here we showed that the levels of insulin receptor substrate-1 phosphorylated at Ser318 and

Ser363/639 were significantly increased in Tg2576 brains; however, after removing one copy of the mTOR gene, the levels of phosphorylated IRS-1 went back to CTL levels. Notably, we previously reported that these changes in insulin receptor substrate-1 phosphorylation in the brain of Tg2576 occur before changes in peripheral insulin signaling (Velazquez et al., 2017). Taken together, these data suggest that hyperactive mTOR may contribute to insulin resistance in AD.

There is a growing appreciation for a role of mTOR signaling in AD pathogenesis (Oddo, 2012). The data presented here show that decreasing mTOR signaling reduces Aβ deposition and levels, which is consistent with previous reports from multiple groups, including our own (Caccamo et al., 2015; Caccamo et al., 2014; Caccamo et al., 2010; Majumder et al., 2011; Spilman et al., 2010; Tramutola et al., 2017). Specifically, we showed that reducing mTOR signaling leads to Aβ and tau reduction by increasing autophagy induction and by decreasing translation of BACE-1 and tau mRNA (Caccamo et al., 2015; Caccamo et al., 2014; Caccamo et al., 2010). We have also shown that Aβ is sufficient to increase mTOR signaling, suggesting a vicious cycle between Aβ and mTOR (Caccamo et al., 2010; Caccamo et al., 2011; Talboom et al., 2015). Despite the strong evidence linking Aβ and mTOR, the mechanisms leading to mTOR hyperactivity in AD remain elusive. mTOR associates with several proteins to form two high molecular weight complexes (known as mTORC1 and mTORC2; (Saxton and Sabatini, 2017). mTORC1 is mainly linked to energy metabolism, cell growth and proliferation while mTORC2 is primarily linked to cytoskeletal organization (Saxton and Sabatini, 2017). The proline-rich Akt substrate 40 (PRAS40) is a key component of mTORC1, and it regulates mTOR activity by physically binding to it. When PRAS40 is bound to mTOR, mTOR activity is reduced; in contrast, when mTOR detaches from PRAS40, mTOR is active (Saxton and Sabatini, 2017). Specifically, insulin signaling facilitates the Akt-mediated phosphorylation of PRAS40 at Thr246. Once phosphorylated, PRAS40 detaches from mTOR, thereby facilitating mTOR activity

(Sancak et al., 2007; Wang et al., 2007). We have previously shown that accumulation of amyloid-β (Aβ) leads to hyperactive mTOR via a PRAS40-mediated mechanism (Caccamo et al., 2011). Given these data and the role of PRAS40 in insulin signaling, it is tempting to speculate that Aβ accumulation increases PRAS40 phosphorylation, which in turn leads to chronic hyperactive mTOR and S6K1 signaling.

It is plausible that factors other than Aβ might trigger mTOR hyperactivity. For instance, diabetes and alterations in insulin signaling are known to directly affect mTOR signaling (Suhara et al., 2017). In turn, as we previously showed, hyperactive mTOR increases Aβ and tau production by altering the expression of BACE-1, a key enzyme in the production of Aβ, and tau (Caccamo et al., 2015). Additionally, hyperactive mTOR decreases turnover of Aβ and tau by reducing autophagy (Orr and Oddo, 2013). While further studies are needed to determine the upstream and downstream mechanisms in this cascade of events, there is an evident interplay between insulin signaling and Aβ and tau (de la Monte, 2012; Diehl et al., 2017; Talbot et al., 2012). For example, high Aβ and tau levels can lead to insulin resistance while insulin dysregulation can also lead to increased Aβ and tau levels (de la Monte, 2012; Diehl et al., 2017; Talbot et al., 2012). Here we show that mTOR is mechanistically linked to such interplay. Consistent with these data, we previously showed that mTOR hyperactivity mediates the detrimental effects of a high sucrose diet on Aβ and tau pathology (Orr et al., 2014).

In summary, we report that insulin dysregulation in Tg2575 mice is mTOR dependent. Furthermore, we present compelling evidence indicating that removing one copy of mTOR in the brain of Tg2576 mice reduces Aβ and tau levels. Notably, there is overwhelming evidence showing that lowering mTOR increases lifespan and health span. Given the role of aging in AD, these data further link mTOR signaling to the pathogenesis of this insidious disorder. Taken

together, these data suggest that reducing mTOR signaling may be a valid therapeutic approach for AD.

Acknowledgements

We thank Mr. Eric Ferreira and Miss An Tran, Arizona State University, for editing the manuscript, Dr. Christopher Lynch, Penn State University College of Medicine, for kindly donating the mTOR floxed mice. This work was supported by grants to S.O. from the Arizona Alzheimer's Consortium and the National Institutes of Health (R01 AG037637).

Declaration of interest

Conflict of interest: None

References

Abner, E.L., Nelson, P.T., Kryscio, R.J., Schmitt, F.A., Fardo, D.W., Woltjer, R.L., Cairns, N.J., Yu, L., Dodge, H.H., Xiong, C., Masaki, K., Tyas, S.L., Bennett, D.A., Schneider, J.A., Arvanitakis, Z., 2016. Diabetes is associated with cerebrovascular but not Alzheimer's disease neuropathology. Alzheimers Dement 12(8), 882-889.

Aguirre-Acevedo, D.C., Lopera, F., Henao, E., Tirado, V., Munoz, C., Giraldo, M., Bangdiwala, S.I., Reiman, E.M., Tariot, P.N., Langbaum, J.B., Quiroz, Y.T., Jaimes, F., 2016. Cognitive Decline in a Colombian Kindred With Autosomal Dominant Alzheimer Disease: A Retrospective Cohort Study. JAMA Neurol 73(4), 431-438.

Alzheimer's, A., 2016. 2016 Alzheimer's disease facts and figures. Alzheimers Dement 12(4), 459-509.

An, W.L., Cowburn, R.F., Li, L., Braak, H., Alafuzoff, I., Iqbal, K., Iqbal, I.G., Winblad, B., Pei, J.J., 2003. Up-regulation of phosphorylated/activated p70 S6 kinase and its relationship to neurofibrillary pathology in Alzheimer's disease. Am J Pathol 163(2), 591-607.

Boura-Halfon, S., Zick, Y., 2009. Phosphorylation of IRS proteins, insulin action, and insulin resistance. Am J Physiol Endocrinol Metab 296(4), E581-591.

Branca, C., Wisely, E.V., Hartman, L.K., Caccamo, A., Oddo, S., 2014. Administration of a selective beta2 adrenergic receptor antagonist exacerbates neuropathology and cognitive deficits in a mouse model of Alzheimer's disease. Neurobiol Aging 35(12), 2726-2735.

Caccamo, A., Branca, C., Talboom, J.S., Shaw, D.M., Turner, D., Ma, L., Messina, A., Huang, Z., Wu, J., Oddo, S., 2015. Reducing Ribosomal Protein S6 Kinase 1 Expression Improves Spatial Memory and Synaptic Plasticity in a Mouse Model of Alzheimer's Disease. J Neurosci 35(41), 14042-14056.

Caccamo, A., De Pinto, V., Messina, A., Branca, C., Oddo, S., 2014. Genetic reduction of mammalian target of rapamycin ameliorates Alzheimer's disease-like cognitive and

pathological deficits by restoring hippocampal gene expression signature. J Neurosci 34(23), 7988-7998.

Caccamo, A., Ferreira, E., Branca, C., Oddo, S., 2017. p62 improves AD-like pathology by increasing autophagy. Mol Psychiatry 22(6), 865-873.

Caccamo, A., Magri, A., Medina, D.X., Wisely, E.V., Lopez-Aranda, M.F., Silva, A.J., Oddo, S., 2013. mTOR regulates tau phosphorylation and degradation: implications for Alzheimer's disease and other tauopathies. Aging Cell 12(3), 370-380.

Caccamo, A., Majumder, S., Richardson, A., Strong, R., Oddo, S., 2010. Molecular interplay between mammalian target of rapamycin (mTOR), amyloid-beta, and Tau: effects on cognitive impairments. J Biol Chem 285(17), 13107-13120.

Caccamo, A., Maldonado, M.A., Majumder, S., Medina, D.X., Holbein, W., Magri, A., Oddo, S., 2011. Naturally secreted amyloid-beta increases mammalian target of rapamycin (mTOR) activity via a PRAS40-mediated mechanism. J Biol Chem 286(11), 8924-8932.

Chang, R.C., Wong, A.K., Ng, H.K., Hugon, J., 2002. Phosphorylation of eukaryotic initiation factor-2alpha (eIF2alpha) is associated with neuronal degeneration in Alzheimer's disease. Neuroreport 13(18), 2429-2432.

Cross, D.A., Alessi, D.R., Cohen, P., Andjelkovich, M., Hemmings, B.A., 1995. Inhibition of glycogen synthase kinase-3 by insulin mediated by protein kinase B. Nature 378(6559), 785-789.

Da Mesquita, S., Ferreira, A.C., Sousa, J.C., Correia-Neves, M., Sousa, N., Marques, F., 2016. Insights on the pathophysiology of Alzheimer's disease: The crosstalk between amyloid pathology, neuroinflammation and the peripheral immune system. Neurosci Biobehav Rev 68, 547-562.

de la Monte, S.M., 2012. Contributions of brain insulin resistance and deficiency in amyloid-related neurodegeneration in Alzheimer's disease. Drugs 72(1), 49-66.

Diehl, T., Mullins, R., Kapogiannis, D., 2017. Insulin resistance in Alzheimer's disease. Transl Res 183, 26-40.

Fenton, T.R., Gout, I.T., 2011. Functions and regulation of the 70kDa ribosomal S6 kinases. Int J Biochem Cell Biol 43(1), 47-59.

Gual, P., Le Marchand-Brustel, Y., Tanti, J.F., 2005. Positive and negative regulation of insulin signaling through IRS-1 phosphorylation. Biochimie 87(1), 99-109.

Hernandez-Sanchez, C., Blakesley, V., Kalebic, T., Helman, L., LeRoith, D., 1995. The role of the tyrosine kinase domain of the insulin-like growth factor-I receptor in intracellular signaling, cellular proliferation, and tumorigenesis. J Biol Chem 270(49), 29176-29181.

Hresko, R.C., Mueckler, M., 2005. mTOR.RICTOR is the Ser473 kinase for Akt/protein kinase B in 3T3-L1 adipocytes. J Biol Chem 280(49), 40406-40416.

Hsiao, K.K., Borchelt, D.R., Olson, K., Johannsdottir, R., Kitt, C., Yunis, W., Xu, S., Eckman, C., Younkin, S., Price, D., et al., 1995. Age-related CNS disorder and early death in transgenic FVB/N mice overexpressing Alzheimer amyloid precursor proteins. Neuron 15(5), 1203-1218.

Kandimalla, R., Thirumala, V., Reddy, P.H., 2017. Is Alzheimer's disease a Type 3 Diabetes? A critical appraisal. Biochim Biophys Acta 1863(5), 1078-1089.

Ke, Y.D., Delerue, F., Gladbach, A., Gotz, J., Ittner, L.M., 2009. Experimental diabetes mellitus exacerbates tau pathology in a transgenic mouse model of Alzheimer's disease. PLoS One 4(11), e7917.

Khurana, V., Lu, Y., Steinhilb, M.L., Oldham, S., Shulman, J.M., Feany, M.B., 2006. TOR-mediated cell-cycle activation causes neurodegeneration in a Drosophila tauopathy model. Curr Biol 16(3), 230-241.

King, G.L., 2008. The role of inflammatory cytokines in diabetes and its complications. J Periodontol 79(8 Suppl), 1527-1534.

Kitazawa, M., Yamasaki, T.R., LaFerla, F.M., 2004. Microglia as a potential bridge between the amyloid beta-peptide and tau. Ann N Y Acad Sci 1035, 85-103.

Kremer, A., Louis, J.V., Jaworski, T., Van Leuven, F., 2011. GSK3 and Alzheimer's Disease: Facts and Fiction. Front Mol Neurosci 4, 17.

Lambon Ralph, M.A., Patterson, K., Graham, N., Dawson, K., Hodges, J.R., 2003. Homogeneity and heterogeneity in mild cognitive impairment and Alzheimer's disease: a cross-sectional and longitudinal study of 55 cases. Brain 126(Pt 11), 2350-2362.

Lang, C.H., Frost, R.A., Bronson, S.K., Lynch, C.J., Vary, T.C., 2010. Skeletal muscle protein balance in mTOR heterozygous mice in response to inflammation and leucine. Am J Physiol Endocrinol Metab 298(6), E1283-1294.

Llorens-Martin, M., Jurado, J., Hernandez, F., Avila, J., 2014. GSK-3beta, a pivotal kinase in Alzheimer disease. Front Mol Neurosci 7, 46.

Ma, T., 2014. GSK3 in Alzheimer's disease: mind the isoforms. J Alzheimers Dis 39(4), 707-710.

Magnuson, B., Ekim, B., Fingar, D.C., 2012. Regulation and function of ribosomal protein S6 kinase (S6K) within mTOR signalling networks. Biochem J 441(1), 1-21.

Majumder, S., Richardson, A., Strong, R., Oddo, S., 2011. Inducing autophagy by rapamycin before, but not after, the formation of plaques and tangles ameliorates cognitive deficits. PLoS One 6(9), e25416.

Menke, A., Casagrande, S., Geiss, L., Cowie, C.C., 2015. Prevalence of and Trends in Diabetes Among Adults in the United States, 1988-2012. JAMA 314(10), 1021-1029.

Oddo, S., 2012. The role of mTOR signaling in Alzheimer disease. Front Biosci (Schol Ed) 4, 941-952.

Orr, M.E., Oddo, S., 2013. Autophagic/lysosomal dysfunction in Alzheimer's disease. Alzheimers Res Ther 5(5), 53.

Orr, M.E., Salinas, A., Buffenstein, R., Oddo, S., 2014. Mammalian target of rapamycin hyperactivity mediates the detrimental effects of a high sucrose diet on Alzheimer's disease pathology. Neurobiol Aging 35(6), 1233-1242.

Ott, A., Stolk, R.P., van Harskamp, F., Pols, H.A., Hofman, A., Breteler, M.M., 1999. Diabetes mellitus and the risk of dementia: The Rotterdam Study. Neurology 53(9), 1937-1942.

Pedersen, W.A., Flynn, E.R., 2004. Insulin resistance contributes to aberrant stress responses in the Tg2576 mouse model of Alzheimer's disease. Neurobiol Dis 17(3), 500-506.

Pei, J.J., Bjorkdahl, C., Zhang, H., Zhou, X., Winblad, B., 2008. p70 S6 kinase and tau in Alzheimer's disease. J Alzheimers Dis 14(4), 385-392.

Pei, J.J., Hugon, J., 2008. mTOR-dependent signalling in Alzheimer's disease. J Cell Mol Med 12(6B), 2525-2532.

Perry, R.J., Hodges, J.R., 1999. Attention and executive deficits in Alzheimer's disease. A critical review. Brain 122 (Pt 3), 383-404.

Querfurth, H.W., LaFerla, F.M., 2010. Alzheimer's disease. N Engl J Med 362(4), 329-344.

Rodriguez-Rivera, J., Denner, L., Dineley, K.T., 2011. Rosiglitazone reversal of Tg2576 cognitive deficits is independent of peripheral gluco-regulatory status. Behav Brain Res 216(1), 255-261.

Sancak, Y., Thoreen, C.C., Peterson, T.R., Lindquist, R.A., Kang, S.A., Spooner, E., Carr, S.A., Sabatini, D.M., 2007. PRAS40 is an insulin-regulated inhibitor of the mTORC1 protein kinase. Mol Cell 25(6), 903-915.

Saxton, R.A., Sabatini, D.M., 2017. mTOR Signaling in Growth, Metabolism, and Disease. Cell 168(6), 960-976.

Schulingkamp, R.J., Pagano, T.C., Hung, D., Raffa, R.B., 2000. Insulin receptors and insulin action in the brain: review and clinical implications. Neurosci Biobehav Rev 24(8), 855-872.

Shinohara, M., Sato, N., 2017. Bidirectional interactions between diabetes and Alzheimer's disease. Neurochem Int.

Sims-Robinson, C., Kim, B., Rosko, A., Feldman, E.L., 2010. How does diabetes accelerate Alzheimer disease pathology? Nat Rev Neurol 6(10), 551-559.

Spilman, P., Podlutskaya, N., Hart, M.J., Debnath, J., Gorostiza, O., Bredesen, D., Richardson, A., Strong, R., Galvan, V., 2010. Inhibition of mTOR by rapamycin abolishes cognitive deficits and reduces amyloid-beta levels in a mouse model of Alzheimer's disease. PLoS One 5(4), e9979.

Steen, E., Terry, B.M., Rivera, E.J., Cannon, J.L., Neely, T.R., Tavares, R., Xu, X.J., Wands, J.R., de la Monte, S.M., 2005. Impaired insulin and insulin-like growth factor expression and signaling mechanisms in Alzheimer's disease--is this type 3 diabetes? J Alzheimers Dis 7(1), 63-80.

Sturchler-Pierrat, C., Abramowski, D., Duke, M., Wiederhold, K.H., Mistl, C., Rothacher, S., Ledermann, B., Burki, K., Frey, P., Paganetti, P.A., Waridel, C., Calhoun, M.E., Jucker, M., Probst, A., Staufenbiel, M., Sommer, B., 1997. Two amyloid precursor protein transgenic mouse models with Alzheimer disease-like pathology. Proc Natl Acad Sci U S A 94(24), 13287-13292.

Suhara, T., Baba, Y., Shimada, B.K., Higa, J.K., Matsui, T., 2017. The mTOR Signaling Pathway in Myocardial Dysfunction in Type 2 Diabetes Mellitus. Curr Diab Rep 17(6), 38.

Talboom, J.S., Velazquez, R., Oddo, S., 2015. The mammalian target of rapamycin at the crossroad between cognitive aging and Alzheimer's disease. NPJ Aging Mech Dis 1, 15008.

Talbot, K., Wang, H.Y., Kazi, H., Han, L.Y., Bakshi, K.P., Stucky, A., Fuino, R.L., Kawaguchi, K.R., Samoyedny, A.J., Wilson, R.S., Arvanitakis, Z., Schneider, J.A., Wolf, B.A., Bennett, D.A., Trojanowski, J.Q., Arnold, S.E., 2012. Demonstrated brain insulin resistance in Alzheimer's disease patients is associated with IGF-1 resistance, IRS-1 dysregulation, and cognitive decline. J Clin Invest 122(4), 1316-1338.

Tramutola, A., Lanzillotta, C., Di Domenico, F., 2017. Targeting mTOR to reduce Alzheimer-related cognitive decline: from current hits to future therapies. Expert Rev Neurother 17(1), 33-45.

Trikkalinou, A., Papazafiropoulou, A.K., Melidonis, A., 2017. Type 2 diabetes and quality of life. World J Diabetes 8(4), 120-129.

Um, S.H., D'Alessio, D., Thomas, G., 2006. Nutrient overload, insulin resistance, and ribosomal protein S6 kinase 1, S6K1. Cell Metab 3(6), 393-402.

Um, S.H., Frigerio, F., Watanabe, M., Picard, F., Joaquin, M., Sticker, M., Fumagalli, S., Allegrini, P.R., Kozma, S.C., Auwerx, J., Thomas, G., 2004. Absence of S6K1 protects against age- and diet-induced obesity while enhancing insulin sensitivity. Nature 431(7005), 200-205.

Vandal, M., White, P.J., Chevrier, G., Tremblay, C., St-Amour, I., Planel, E., Marette, A., Calon, F., 2015. Age-dependent impairment of glucose tolerance in the 3xTg-AD mouse model of Alzheimer's disease. FASEB J 29(10), 4273-4284.

Velazquez, R., Tran, A., Ishimwe, E., Denner, L., Dave, N., Oddo, S., Dineley, K.T., 2017. Central insulin dysregulation and energy dyshomeostasis in two mouse models of Alzheimer's disease. Neurobiol Aging 58, 1-13.

Wang, L., Harris, T.E., Roth, R.A., Lawrence, J.C., Jr., 2007. PRAS40 regulates mTORC1 kinase activity by functioning as a direct inhibitor of substrate binding. J Biol Chem 282(27), 20036-20044.

Figure Legends

Figure 1: Reduced mTOR signaling improves learning and memory in the APP/mTOR$^{+/-}$ mice. A, Learning curve of 20-month-old mice trained in the spatial reference version of the MWM. Mice were trained for five days to swim to find a hidden platform using extramazal visual cues. Each day represents the average of four training trials. All genotypes significantly learned the task; however, APP mice took more time to find the platform on day 4 and day 5. **B**-**C**, Memory, was tested 24 h after the last training trial. The APP mice were significantly impaired compared with the other three genotypes. Remarkably, the APP/mTOR$^{+/-}$ mice performed as well as the WT mice in both the parameter analyzed. **D,** Swim speed measured during the probe trials was not statistically different among the four genotypes. *n* = 10/genotype, 5 females and 5 males. Data are presented as means ± SEM and were analyzed by two-way ANOVA with Bonferroni's correction.

Figure 2: Reduced mTOR levels and signaling in APP/mTOR$^{+/-}$ mice. A, Weight of mice at the time of death. There were no statistically significant changes for any of the genotypes ($p = 0.4028$). **B**, Representative western blots of proteins extracted from the cortices of 20-month-old mice probed with the indicated antibodies. **C-E**, Quantification of the blots indicates a significant decrease in the levels of mTOR and phospho-S6K1 in APP/mTOR$^{+/-}$ and mTOR$^{+/-}$ mice compared to the other two groups ($p < 0.0001$; $p = 0.0051$, respectively). Levels of total S6K1 were unchanged ($p = 0.3084$). Data were obtained by normalizing the protein of interest to β-actin loading control. Results presented as means ± SEM and analyzed by one-way ANOVA with Bonferroni's correction. Panel A, n = 10 mice/genotype (5 females and 5 males); Panels B-E, n = 5 mice/genotype (3 females and 2 males). * indicates that the APP and the CTL groups are significantly different compared to the other two groups.

Figure 3: Low mTOR rescues aberrant insulin signaling in APP mice. A, Representative western blots of protein extracted from CTL, mTOR$^{+/-}$, APP and APP/mTOR$^{+/-}$ mice probed with the indicated antibodies. **B**, Quantification of IRβ levels shows a decrease in the levels of this protein in the APP mice compared to the other genotypes ($p < 0.0001$). **C,** Levels of total IRS were unchanged among the groups ($p = 0.9118$). **D-E**, Levels of IRS-1 phosphorylated at Ser318 ($p = 0.0093$) and Ser636/639 ($p = 0.0304$) were significantly higher in the APP mice compared to the other groups (n = 5 mice/genotype). **F-G**, Sandwich ELISA measurements of total IGF-1R and phospho-IGF-1R. Both proteins were lower in the APP/mTOR$^{+/-}$ mice compared to the APP mice ($p < 0.0001$ and $p = 0.0033$, respectively) n = 5 mice/genotype, 3 females and 2 males. Data were obtained by normalizing the protein of interest to β-actin loading control. Results presented as means ± SEM and analyzed by one-way ANOVA with Bonferroni's correction.

Figure 4: Reduced mTOR signaling rescues the aberrant activation of the PI3K/AKT pathway. A, Representative western blots of protein extracted CTL, mTOR$^{+/-}$, APP and APP/mTOR$^{+/-}$ mice probed with the indicated antibodies. **B-C**, Quantification of the total and phospho levels of Pi3K. While the levels of total PI3K remain unchanged among the groups, there was a significant increase in phospho-PI3K in the APP compared to the other three genotypes ($p = 0.7921$ and $p = 0.0036$, respectively). **D-F**, Quantification of total and phospho-AKT. The level of total AKT remains unaltered in the four groups ($p = 0.1115$), while the levels of AKT Thr308 and AKT Ser473 were decreased in the APP/mTOR$^{+/-}$ compared to APP mice ($p = 0.0063$ and $p = 0.0075$, respectively). The graphs were generated by normalizing the protein of interest to β-actin loading control. Results presented as means ± SEM and analyzed by one-way ANOVA with Bonferroni's correction. For each experiment shown, *n* = 5 mice/genotype, 3 females and 2 males. * indicates that the APP group was significantly different compared to the other three groups.

Figure 5: Reducing aberrant mTOR signaling lowers Aβ levels in APP/mTOR$^{+/}$ mice. A, Representative cortical sections from APP and APP/mTOR$^{+/-}$ mice stained with an Aβ42-specific antibody. **B,** Quantitative analysis of the section showed a significant reduction in number of plaques in APP/mTOR$^{+/-}$ mice ($p < 0.0001$). **C,** Representative western blot of protein from APP and APP/mTOR$^{+/-}$ mice probed with the indicated antibodies. **D-F**, Quantitative analyses showed that APP, C99 and C83 levels were similar between APP and APP/mTOR$^{+/-}$ mice ($p = 0.1831$, $p = 0.2945$ and $p = 0.4524$, respectively). **G**, Measurements of soluble $A\beta_{42}$ and $A\beta_{40}$ by sandwich ELISA. The levels of both peptides were lower in the APP/mTOR$^{+/-}$ mice compared to APP ($p = 0.0003$ and $p = 0.0004$, respectively). **H,** Measurements of insoluble $A\beta_{42}$ and $A\beta_{40}$ by sandwich ELISA. The levels $A\beta_{42}$ were lower in the APP/mTOR$^{+/-}$ mice compared to APP while the levels of $A\beta_{40}$ were unchanged ($p = 0.0002$ and $p = 0.5982$, respectively). Data were obtained by normalizing the protein of interest to β-actin loading control and analyzed by Student's *t*-test. Panels A-F: n = 5/genotype, 3 females and 2 males; Panel G-H: n = 6/genotype, 3 females and 3 males.

Figure 6: Reduced endogenous tau levels in APP/mTOR$^{+/-}$ mice. A, Representative western blot of protein from CTL, mTOR$^{+/-}$, APP and APP/mTOR$^{+/-}$ mice probed with the indicated antibodies. **B**, Quantitative analysis of total mouse tau indicated that endogenous tau levels were decreased in APP/mTOR$^{+/-}$ compared to the APP mice ($p = 0.0068$). **C**, Quantitative analysis of phosphorylated tau using CP13, an antibody that recognizes tau phosphorylated at Ser202. The levels of this protein were reduced in APP/mTOR$^{+/-}$ compared to the APP mice ($p = 0.0027$). **D**, Quantitative analysis of phosphorylated tau using PHF-1, an antibody that recognizes tau phosphorylated at Ser396/404. No changes were detected in the levels of this protein among the four genotypes ($p = 0.1343$). **E-F**, Quantification of total and phospho-

GSK3β. The levels of total GSK3β were the same for all genotypes (p = 0.9770). Phospho-GSK3β levels were higher in the APP/mTOR$^{+/-}$ compared to the APP mice (p < 0.0001). Data were obtained by normalizing the protein of interest to β-actin loading control. Results presented as means ± SEM and analyzed by one-way ANOVA with Bonferroni's correction. For each experiment shown, *n* = 5 mice/genotype, 3 females and 2 males. * indicates that the APP group was significantly different compared to the other three groups.

Figure 7: Decrease of pro-inflammatory cytokine in APP/mTOR$^{+/-}$ mice. A, Representative western blot of protein from CTL, mTOR$^{+/-}$, APP and APP/mTOR$^{+/-}$ mice probed with the indicated antibodies. **B**, Quantitative analysis of IL1β. The graph shows that the levels of IL1β were reduced in the APP/mTOR$^{+/-}$ compared to the APP mice (p = 0.0010). **C**, Quantitative analysis of TNFα. The graph shows that the levels of TNFα were lower in the APP/mTOR$^{+/-}$ compared to the APP mice (p = 0.0206). Data were obtained by normalizing the protein of interest to β-actin loading control. Results presented as means ± SEM and analyzed by one-way ANOVA with Bonferroni's correction. For each experiment shown, *n* = 5 mice/genotype, 3 females and 2 males.

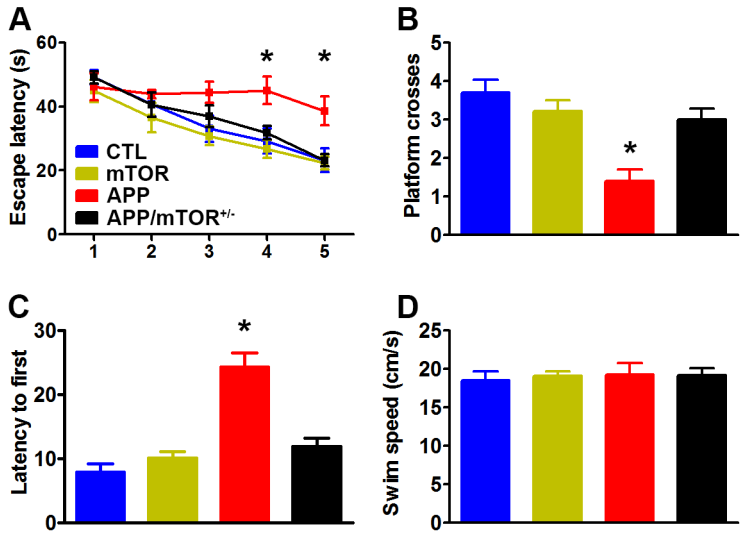

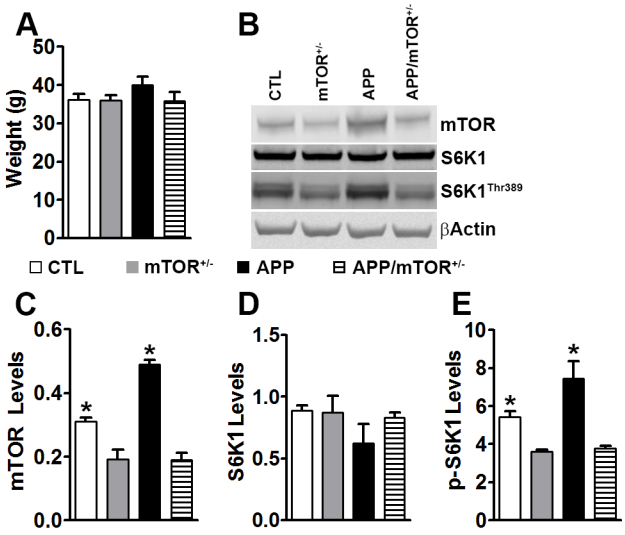

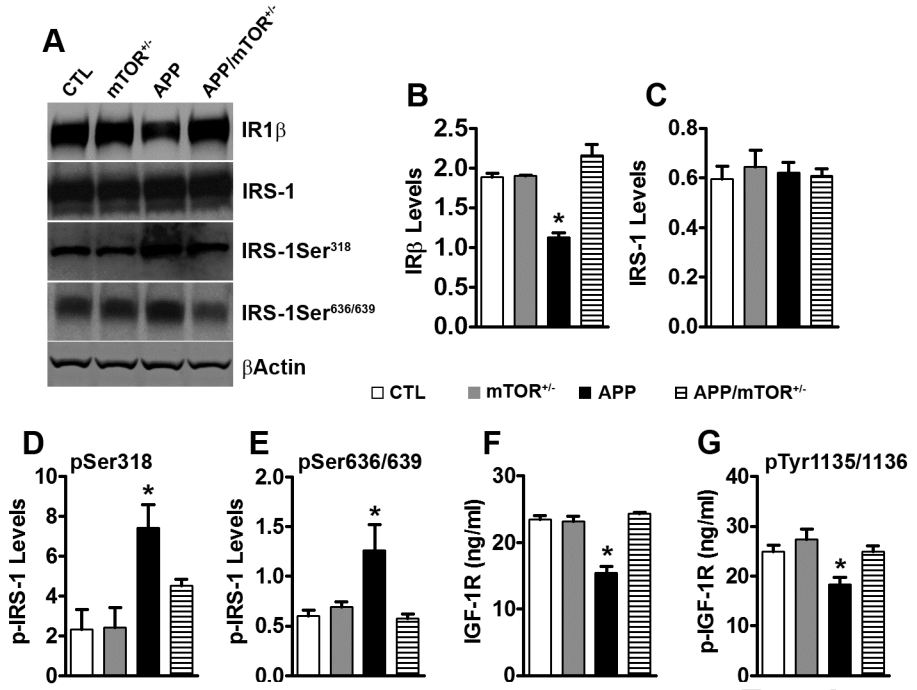

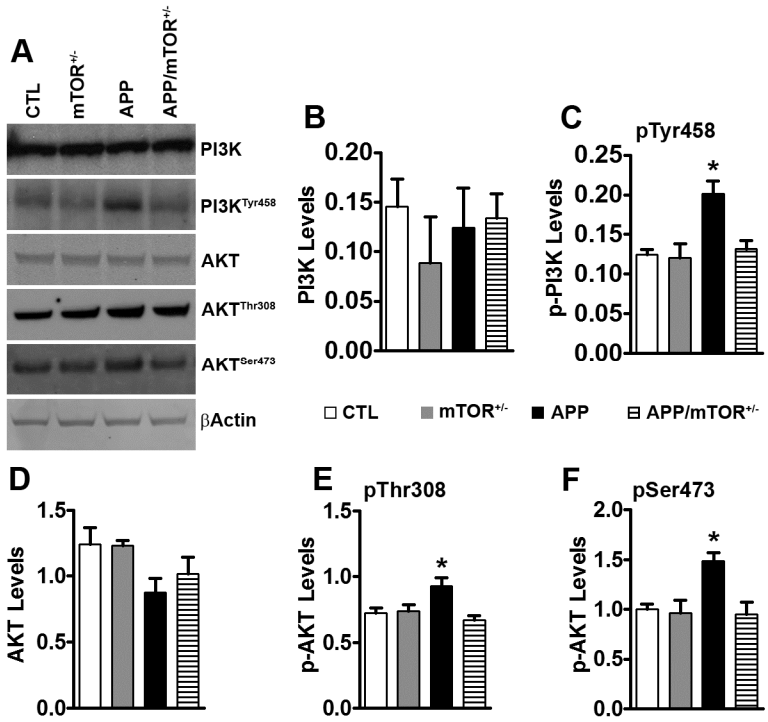

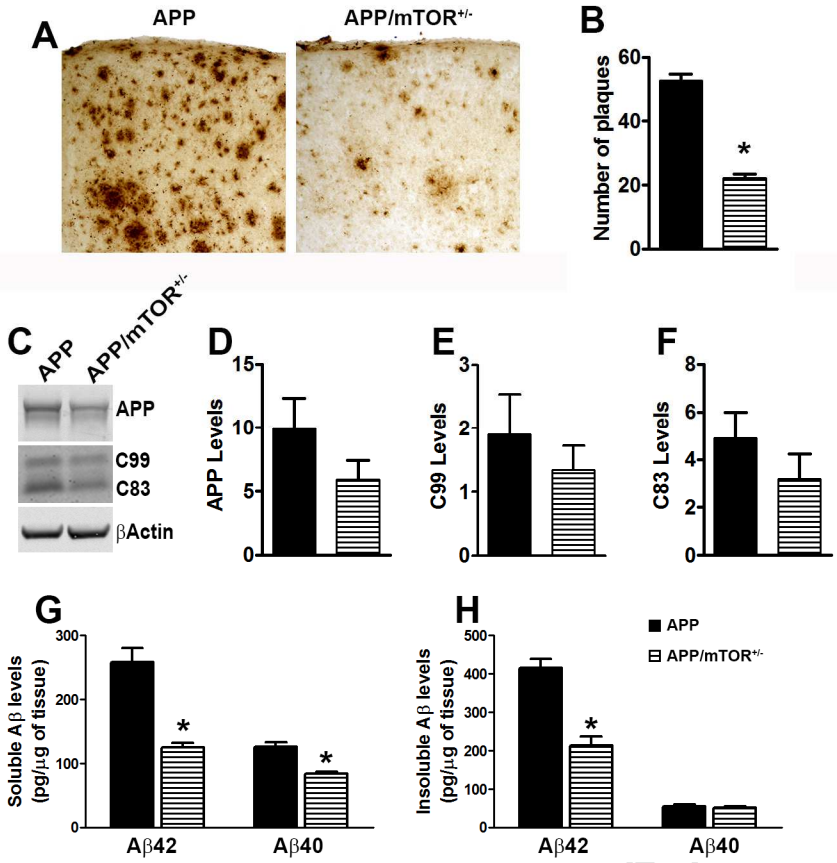

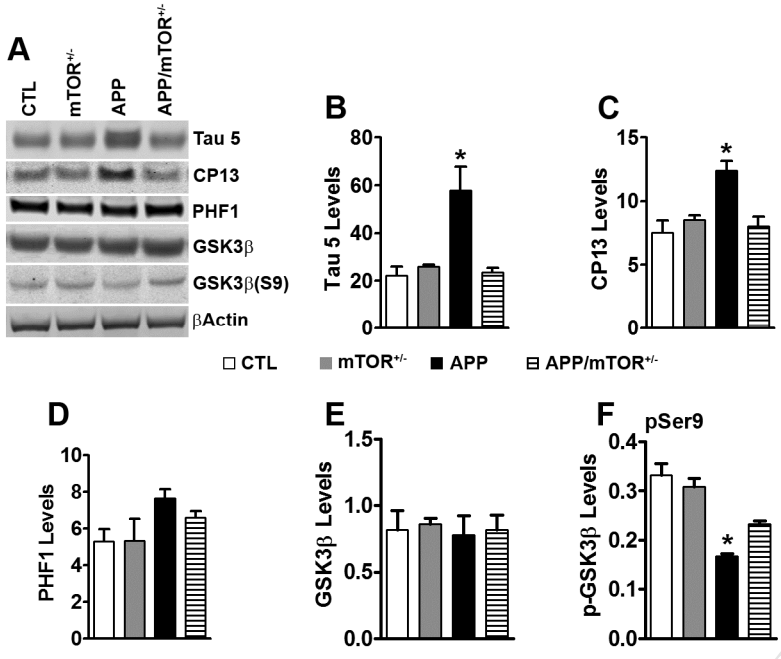

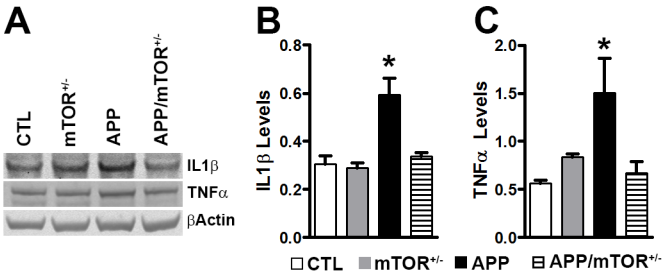

Highlights

- Reducing brain mTOR signaling improves central insulin dysregulation in 20-month-old Tg2576 mice
- Reducing brain mTOR signaling lowers Aβ and tau levels in 20-month-old Tg2576 mice
- Reducing brain mTOR signaling lowers cytokines levels in 20-month-old Tg2576 mice.
- Hyperactive mTOR may contribute to AD-like pathology in 20-month-old mice.